Power-Up SRAM State as an Identifying Fingerprint and Source of True Random Numbers

Daniel E. Holcomb, *Student Member*, *IEEE*, Wayne P. Burleson, *Senior Member*, *IEEE*, and Kevin Fu, *Member*, *IEEE*

Abstract—Intermittently powered applications create a need for low-cost security and privacy in potentially hostile environments, supported by primitives including identification and random number generation. Our measurements show that power-up of SRAM produces a physical fingerprint. We propose a system of Fingerprint Extraction and Random Numbers in SRAM (FERNS) that harvests static identity and randomness from existing volatile CMOS memory without requiring any dedicated circuitry. The identity results from manufacture-time physically random device threshold voltage mismatch, and the random numbers result from runtime physically random noise. We use experimental data from high-performance SRAM chips and the embedded SRAM of the WISP UHF RFID tag to validate the principles behind FERNS. For the SRAM chip, we demonstrate that 8-byte fingerprints can uniquely identify circuits among a population of 5,120 instances and extrapolate that 24-byte fingerprints would uniquely identify all instances ever produced. Using a smaller population, we demonstrate similar identifying ability from the embedded SRAM. In addition to identification, we show that SRAM fingerprints capture noise, enabling true random number generation. We demonstrate that a 512-byte SRAM fingerprint contains sufficient entropy to generate 128-bit true random numbers and that the generated numbers pass the NIST tests for runs, approximate entropy, and block frequency.

Index Terms—SRAM, chip ID, TRNG, RFID.

1 Introduction

Identification and random number generation are important primitives in integrated circuits. A static identifier is a collection of bits that does not change over time and can be used to differentiate instances of logically identical circuits. A true random number is a collection of bits that are unpredictable and show statistical properties of randomness. Random numbers are essential in applications such as key generation. If the numbers can be guessed with any accuracy, the security of any scheme that relies on them is broken, as was exploited in Goldberg and Wagner's attack on the Netscape SSL implementation [1]. To support resource-constrained integrated circuits being used in security-critical applications such as contactless credit cards [2] and pacemakers [3], it is important to accomplish both identification and random number generation at minimal cost and without sacrificing quality.

1.1 Contribution of This Work

Our method of Fingerprint Extraction and Random Numbers in SRAM (FERNS) uses volatile CMOS memory for chip identification and true random number generation (TRNG). The major contributions of this work are demonstrating that the power-up of SRAM reveals a physical fingerprint of the chip and demonstrating that this fingerprint can provide identification and TRNG at low hardware cost, even in applications lacking circuits dedicated to either purpose. The fingerprints are generated incidentally in intermittently powered passive and mobile devices as they are powered-up before use. The cost constraints that are often associated with these applications create an ideal platform for FERNS, as demonstrated by an early version of this work that targeted exclusively RFID applications [4].

1.2 Summary of Experimental Methodology

The FERNS method is validated through experiments on two platforms. The first is a population of 512-Kbyte SRAM chips [5], powered and read out using Altera's DE2 development board [6]. The second platform is a population of embedded SRAMs, each on board one of Intel's wirelessly powered platform for sensing and computation, or WISPs [7], [8], [9]. The WISP is an RFID device, passively powered at 915 MHz in the ultrahigh frequency band. It transmits data in 64-bit packets according to the Electronic Product Code Gen 1 specification [10], allowing communication with commercially available RFID readers. The embedded SRAM on the WISP is the 256-byte memory of an ultralow power Texas Instruments MSP430F1232 microcontroller [11]. The SRAM chip and embedded SRAM are designed according to opposing objectives and present the opportunity to explore how a variety of factors might influence SRAM fingerprints. The memory of the SRAM chip is designed for high performance, is not power constrained, and is free from surrounding logic circuitry that could interfere with fingerprints. In contrast, the

- *D.E. Holcomb is with the University of California, Berkeley, CA 94702. E-mail: holcomb@eecs.berkeley.edu.*
- *W.P. Burleson and K. Fu are with the University of Massachusetts, Amherst, MA 01003. E-mail: burleson@ecs.umass.edu, kevinfu@cs.umass.edu.*

Manuscript received 1 Nov. 2007; revised 23 June 2008; accepted 7 Oct. 2008; published online 7 Nov. 2008.
Recommended for acceptance by R. Stenwandt, W. Geiselmann, and C.K. Koc. For information on obtaining reprints of this article, please send e-mail to: tc@computer.org, and reference IEEECS Log Number TCSI-2007-11-0549.
Digital Object Identifier no. 10.1109/TC.2008.212.

embedded SRAM on the WISP is designed for low performance and low leakage, is passively powered, and is near the data path and control circuitry. Our experiments on these two platforms show that otherwise identical circuits can be identified using only SRAM fingerprints and that numbers generated from fingerprints can pass basic statistical tests for randomness.

The remainder of this paper is organized as follows: Section 2 provides related work in identification and random number generation. Section 3 gives the physical foundations for the FERNS method. Sections 4 and 5 present results of fingerprint identification and TRNG, respectively. Section 6 analyzes the robustness of the FERNS method with respect to environmental changes, and Section 7 concludes this paper.

2 Related Work

FERNS provides both identification and randomness using the power-up state of SRAM cells. Thus, the principles behind FERNS are related to works in both physical identification circuits and TRNG circuits.

2.1 Identification

Circuits can be identified through the use of either nonvolatile memories or some distinctive physical characteristic. The nonvolatile approach involves programming an identifier into the circuit using EPROM, EEPROM, flash, fuse, or other strategies. While identifiers stored in nonvolatile memories are static and reliable, they have drawbacks including 1) trivial clonability; 2) the area cost of supporting circuitry such as charge pumps for tunneling oxide devices and programming transistors for fuse devices; and 3) the cost of additional process steps required to implement nonvolatile technologies [12]. Even if minimal nonvolatile storage is desired, the process costs must be paid across the entire chip area. More relevant to the FERNS method are existing works that overcome some of the drawbacks of using nonvolatile memory for identification; these approaches can be classified as either physical fingerprinting or physical unclonable functions (PUFs). Physical fingerprinting is a method for distinguishing circuits according to some physical characteristic—an electronic analog of human fingerprinting. PUFs use physical characteristics for challenge-response authentication.

2.1.1 Physical Fingerprinting

Physical fingerprint identification uses the inherent process variation of integrated circuits to differentiate instances of logically identical chips. The fingerprints are generated using standard CMOS fabrication processes, and have greater resistance to cloning than nonvolatile IDs. The primary drawback to physical fingerprint identification is that fingerprints can be influenced by noise and environment.

Process variation comes in many forms, including lithography-induced variations in feature size and random threshold voltage assignment due to dopant fluctuations. Because lithographic variations are spatially correlated [13] and dopant fluctuations are not [14], threshold assignment is the preferred identifying characteristic. Furthermore, threshold voltage variation is expected to increase as MOSFET channel geometries shrink with continued technology scaling [15]. Threshold assignment can be used to generate identifying fingerprints in many ways. An early example indirectly measures MOSFET threshold voltages for RFID identification [16]. A second approach uses threshold voltage mismatch to resolve contention between cross-coupled NOR cells in an identifying way [17]; this work is very similar to SRAM fingerprinting and is revisited in detail in Section 4.3. The important difference between these designs and our work is that the FERNS method obtains its physical fingerprint identities from existing SRAM arrays, instead of using special purpose circuitry to generate the ID.

Although unbeknownst to us while developing this work, we have since discovered a 2002 patent on the electronic fingerprinting of semiconductor integrated circuits using SRAM [18]. No associated experimental data was ever published, and the patent does not mention the random number generating capabilities of SRAM.

2.1.2 Physical Uncloneable Functions

Silicon PUFs map input challenges to output responses using a function determined by the inherent variations of each chip. As the variation determines the mapping, it is effectively the "key" to the PUF. Unclonability results from the uncontrollability of the variations, which prevent an adversary from duplicating an existing PUF instance, given some reasonable assumptions regarding the adversary's capabilities. Like algorithmic one-way hash functions, the mapping of PUFs should be simple to compute in the forward direction but infeasible to invert.

The arbiter PUF uses an input-controlled race condition and produces a response based on the relative delays of the racing paths [22]. The same arbiter PUF design is used for TRNG by finding and then persistently applying specific inputs that cause races between well-matched paths, leading to unpredictable outcomes [23].

Closely related to the FERNS method presented in this paper is a PUF design for FPGAs that uses a derivative of power-up SRAM state as a secret key to an algorithmic one-way hash function [24], [25]. While this work was published after our initial work on SRAM fingerprinting [4], we point out to readers that it was developed concurrently and independently of our work. The use of the hash function allows the SRAM PUF to provide challenge-response authentication that FERNS does not, but also requires that a reliable secret key be obtained from the noisy power-up SRAM state. Generating this key requires that helper data be provided to manipulate the SRAM state into a redundant code word so that error correction can be applied; 4,600 bits of SRAM are required to generate a single 128-bit secret. To keep the key secret, these SRAM bits cannot be used as memory. The memory cost of the SRAM PUF is excessive if challenge-response authentication is not necessary, as the FERNS method provides 128 bits of ID using less than 680 bits of SRAM (Table 1) with no restriction against using the SRAM as memory after identification.

2.2 Random Number Generation

Approaches to creating random numbers can be broadly classified as either TRNG or pseudorandom number generation (PRNG). TRNG designs rely on a random physical process, whereas PRNG designs use deterministic algorithms to generate periodic sequences of numbers that have statistical properties of randomness; only TRNG is

TABLE 1
Comparing FERNS SRAM ID with the Two Layouts of Related Work

	Su et al. [17]		FERNS	
	Symmetric	**Common Centroid**	**SRAM Chip**	**WISP**
Transistors per cell	10	20	6	6
Approximate area per cell in 0.13μ technology (μm^2)	40	80	3	3
Fractional Hamming Distance	0.505	0.501	0.417	0.469
$ID_{bits}/cell$	< 1	< 1	≥ 0.19	≥ 0.06
Area per ID bit (μm^2)	≥ 40	≥ 80	≤ 15.8	≤ 50.0

The SRAM chip statistics are based on 100 latent fingerprints from each device, while the embedded SRAM statistics are based on 16 latent fingerprints from each device. Cell areas for SRAM in 0.13-μm technology are estimated [32].

considered in this work. Most TRNG designs use thermal noise as the random process. Thermal noise in integrated circuits describes small voltage fluctuations that exist on conductors in equilibrium [26], [27]. Generating random bits from thermal noise requires some process that is influenced by the noise. One well-known mechanism is to detect its manifestation in the jitter of free-running oscillators [28]. A second mechanism to detect thermal noise is to amplify it to a measurable level using direct amplification or the large gain that exists in metastable CMOS devices [29]. A work that is closely related to the FERNS method also uses the high gain of metastable cross-coupled CMOS devices as the mechanism to detect thermal noise [30]; this design is revisited in detail in Section 5.2. An important difference between the aforementioned TRNG designs and the FERNS method is that FERNS generates random bits using the power-up of existing SRAM arrays, instead of a dedicated circuit.

3 SRAM as a Physical Fingerprint

FERNS builds upon the observation that the power-up of SRAM cells reveals a physical fingerprint. With an SRAM cell being the required circuitry for storing and accessing a bit, each cell is perhaps the smallest possible physical fingerprint circuit that can produce a digital output. The remainder of this section presents the FERNS method, starting at the circuit level by identifying why SRAM power-up generates a physical fingerprint.

3.1 Principles of FERNS

Each bit of SRAM is a six-transistor memory cell, consisting of cross-coupled CMOS inverters and access transistors [31]. Each of the inverters drives one of the two state nodes, labeled "A" and "B" in Fig. 1. When the circuit is unpowered, both state nodes are discharged low $(\mathrm{AB} = 00)$. When power is applied, this unstable state will transition to one of the two stable states, either "0" $(\mathrm{AB} = 01)$ or "1" $(\mathrm{AB} = 10)$; the $\mathrm{AB} = 11$ state is unstable and unreachable. The tendency to transition to one state or the other depends on process variation mismatch and noise. Because the stabilization of each cell depends only on differences between local devices, the impacts of common-mode process variations such as lithography and common-mode noise sources such as supply fluctuations and substrate temperature are minimized (see Section 6).

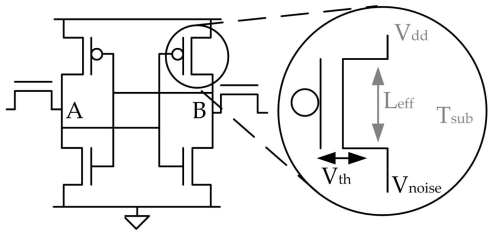

Fig. 1. SRAM cell with relevant process variation and noise shown. Threshold voltage mismatch is the source of ID and varies from cell to cell. Noise is the source of randomness.

For illustrative purposes, both process variation and noise are considered as impacting the "skew" of a cell. The skew of a cell is a continuous quantity used to represent the power-up tendency of that cell. Skew at a given power-up is influenced by noise, so the skew of each cell across many power-ups is described by a probability distribution function (Fig. 2). A 0-skewed or 1-skewed cell will power-up to 0 or 1, respectively, regardless of noise conditions (Fig. 2a). A neutral-skewed cell does not have a strong tendency toward either state and can power-up to either 0 or 1 (Fig. 2b). A neutral-skewed cell does not necessarily consist of perfectly matched devices, but instead has some unknowable combination of variations that are approximately offsetting when powered-up under nominal conditions; this distinction is significant as it indicates that such a cell may not remain neutral across all operating conditions. Note that the ternary classification of cells as clearly either 0-skewed, 1-skewed, or neutral-skewed is an illustrative simplification only.

3.2 Latent versus Known Physical Fingerprints

We define a physical fingerprint of an SRAM array to be the power-up state generated by its constituent SRAM cells.

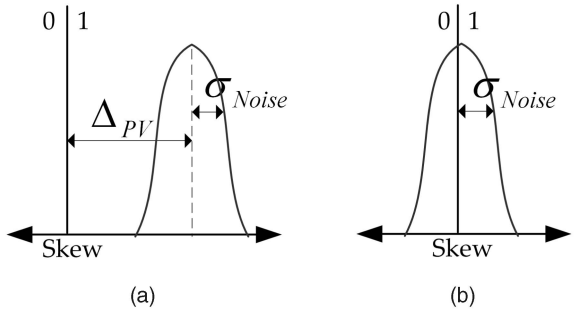

Fig. 2. If a cell is strongly 0-skewed or 1-skewed, the minor influence of noise is insufficient to sway power-up state; such cells provide identification. If a cell is neutral-skewed, the influence of noise can determine its power-up state; such cells provide randomness. (a) Tendencies of 1-skewed cell. (b) Tendencies of neutral-skewed cell.

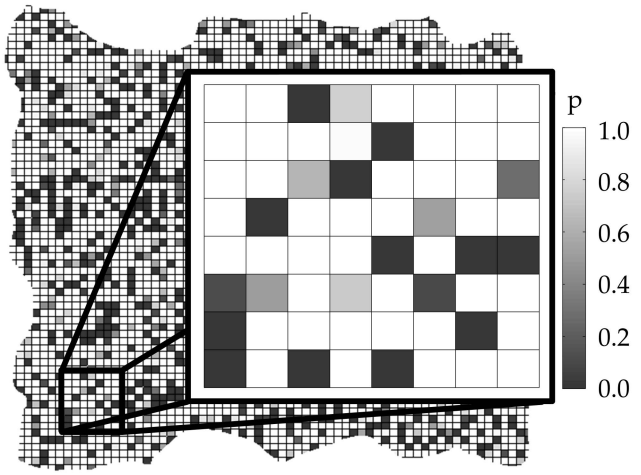

Fig. 3. A 64-bit fingerprint, shown within a larger fingerprint for context. The lightness of the shading of each cell indicates p, the probability of powering-up to 1, as measured over 100 trials. A 64-bit fingerprint can identify an SRAM chip among a population of 5,120.

Some of the cells in the array are neutral-skewed and unreliable across power-up trials, adding randomness to a fingerprint. Other cells are 0-skewed or 1-skewed but not correlated to the same bits on different chips, acting as reliable identifying features of a fingerprint. Thus, an SRAM physical fingerprint is a fuzzy identifier of a chip Fig. 3, much as a literal fingerprint is a fuzzy identifier of a human. Borrowing terminology from human fingerprinting, the terms latent and known fingerprints are defined as follows:

A **latent fingerprint** is an SRAM fingerprint produced at a single power-up. With $l(i)$ denoting the state of a single SRAM cell at power-up i, an N-bit latent fingerprint is simply the collective state of a specified set of N cells at power-up i:

$$L_C = \{l_0(i), l_1(i), \ldots, l_N(i)\}. \quad (1)$$

As a latent fingerprint is sensitive to noise, and some bits will not power-up to their most probable state, the same set of SRAM cells can produce many different latent fingerprints.

A **known fingerprint** is an intentional estimation of the state that a given set of SRAM cells is most likely to generate at power-up and is used as the known identity of a chip. The most likely power-up state of each cell is determined by averaging across an odd number of trials

$$p = \underset{\forall i}{avg}(l(i)) \quad (2)$$

and rounding to a binary value k

$$k = \left\{ \begin{array}{ll} 0 & \text{if } p < 0.5 \\ 1 & \text{if } p > 0.5 \end{array} \right\}. \quad (3)$$

Averaging over multiple power-ups reduces the impact of noise, making a known fingerprint more representative of the SRAM cells that generate it than a latent fingerprint from the same cells:

$$K_C = \{k_0, k_1, \ldots, k_N\}. \quad (4)$$

The differences between latent and known fingerprints imply their usage in the FERNS method of identification and random number generation. Identification is enabled by the similarity between known and latent fingerprints when both are generated by the same chip, compared to the lack of similarity between those generated by different chips. TRNG is possible because the minor differences between latent fingerprints generated by the same chip cause large latent fingerprints to be effectively unique.

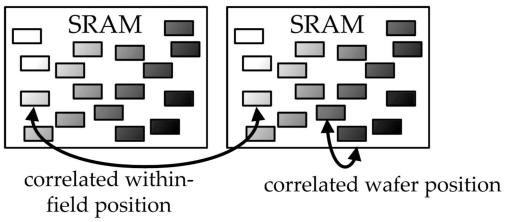

Fig. 4. Physical devices are partitioned into logical devices, shown shaded according to their within-field position. The use of logical devices allows for comparison of SRAM fingerprint IDs from both correlated within-field positions and correlated wafer positions.

4 FERNS for Identification

FERNS determines identity from SRAM physical fingerprints using a simple Hamming distance matching. A single known fingerprint is first created for each chip that is to be identified and stored in a database. When a latent fingerprint of unknown origin is obtained, its Hamming distance to each known fingerprint is determined:

$$HD(L_C, K_{Cj}) = L_C \oplus K_{Cj}. \quad (5)$$

The correct identity of the chip that produced the latent fingerprint is determined from the known fingerprint with the closest Hamming distance to it:

$$ID(L_C) = K_{Cj} \in \{\forall K_C\} : HD(L_C, K_{Cj}) \text{ is minimized.} \quad (6)$$

If this known fingerprint does in fact come from the same chip as the latent fingerprint, then the identification is deemed successful.

Two distributions are used to characterize and demonstrate the quality of the fingerprints:

1. The distribution of Hamming distances between latent fingerprint and known fingerprint when both are generated by the same chip. A close distance indicates a reliable fingerprint.
2. The distribution of Hamming distances between latent fingerprint and all known fingerprints not generated by the same chip. A large distance indicates a low probability of false identification.

4.1 Logical Devices

To evaluate the identifying properties of SRAM, physical fingerprints with potentially correlated process variation are compared through the use of logical devices. The logical devices occupy the same addresses across all chips. Logical devices that occupy the same positions on different chips have correlated within-field positions, while logical devices from nearby locations on the same chip have correlated wafer positions (Fig. 4). If fingerprint identities are influenced by lithographic mask variation, those generated from correlated

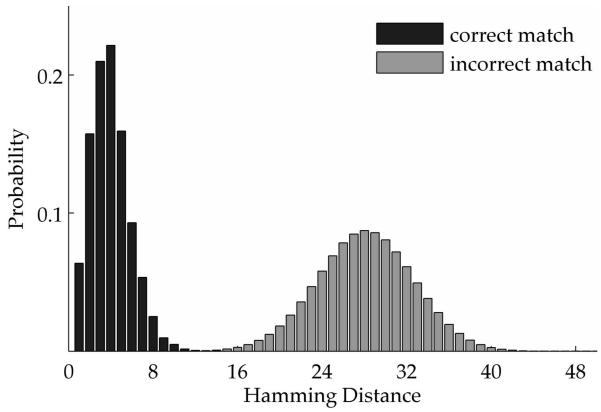

Fig. 5. In the SRAM chip, the Hamming distances between latent and known fingerprints generated by the same logical devices are closer than those generated by different devices, enabling fingerprint identification.

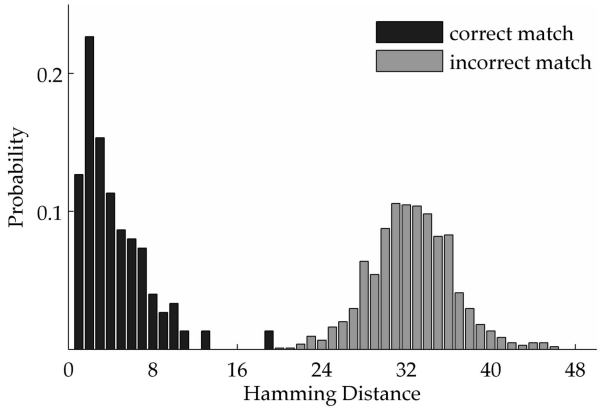

Fig. 6. In the embedded SRAM, the Hamming distances between latent and known fingerprints generated by the same logical device are generally closer than those generated by different devices, enabling fingerprint identification.

within-field positions may be similar. Alternatively, if fingerprint identities are influenced by wafer-level processing steps, those generated from correlated wafer positions may be similar. Without logical devices, there would be no way to determine the relative wafer positions of the packaged chips being compared. For the SRAM chip design, 5,120 logical devices are used for identification, distributed across eight packaged chips. For the embedded SRAM design, 15 logical devices are used, across three chips. It is observed that neither logical devices having correlated wafer positions nor those having correlated within-field positions generate fingerprints showing a strong correlation.

4.2 Analysis of Fingerprint Matching Results

For both the SRAM chip and the embedded SRAM, the identifying ability of fingerprints is demonstrated using logical devices. For each platform, the known fingerprints are created by averaging over three power-ups. Additional power-up trials then generate latent fingerprints to identify.

4.2.1 SRAM Chip

Hamming distance identification performed on two latent fingerprints from each of the 5,120 64-bit SRAM logical devices is found to be 100 percent reliable. For each of the 10,240 latent fingerprints being identified, the identity determined by the matching algorithm (out of 5,120 possibilities) was the correct one each time. If the sizes of the fingerprints are reduced to 32 bits, the success rate of the identification drops to 96 percent.

The expected Hamming distance for a correct match of latent to known fingerprint is 2.45 (Fig. 5). We expected the Hamming distance between incorrect matchings to be centered at 32 bits but instead observed a slight yet consistent pathology whereby measurements were centered at 27.62. This slight similarity does not seem due specifically to correlated locations of 1-skewed cells and 0-skewed cells across chips but instead appears due to a majority of all cells being 1-skewed. Potential causes of this include asymmetry in the SRAM design or the fabrication process.

4.2.2 Embedded Microcontroller SRAM

Hamming distance identification on 16 latent fingerprints from each of the 15 embedded SRAM logical devices produces a 100 percent accurate matching. The embedded SRAM fingerprints are noisier than those of the SRAM chip, as reflected in the expected Hamming distance of 4.12 between latent and known fingerprints for a correct match. The reason for this is undetermined; it is hypothesized to be attributable to differences in technologies used, the influence of neighboring circuitry, or both. The expected Hamming distance between latent and known fingerprints that constitutes an incorrect match is 31.58 (Fig. 6). Reducing the size of the fingerprints to 32 bits reduces the success rate of the matching to 99 percent.

Note that some correct matchings show an unusually large Hamming distance of 18 bits (Fig. 6). Upon inspection, these cases result from latent fingerprints that contain long strings of 1s and 0s that are uncorrelated to the known fingerprint of that embedded SRAM device. These outlying fingerprints are believed to be caused by remanance; subsequent work shows that the WISP platform can retain values stored in RAM for tens of seconds after being powered down [48].

4.2.3 Quantifying the Identity Content of Fingerprints

The sizes of the populations for which successful identification is demonstrated provides an estimated lower bound on the amount of identifying information contained in the fingerprints:

$$ID_{bits}/fingerprint \geq \log_2(|Identified\ Population|). \quad (7)$$

The number of bits of identifying information is equivalent to the minimum number of perfectly reliable ID bits required for unique identification in a population of the same size. This gives a lower bound because there is only a lower bound on the maximum population size that can be identified using 64 bits; while our experiments only used populations of size 5,120 and 15 for the two platforms, it is possible that 64-bit fingerprints would be able to provide successful identification among larger populations. By demonstrating successful identification of circuits from among a population of 5,120, each 64-bit SRAM chip fingerprint is shown to provide at least 12.3 bits of ID, or 0.192 bits of ID per cell:

$$ID_{bits}/cell = \frac{ID_{bits}/fingerprint}{N_{bits\ in\ fingerprint}}. \quad (8)$$

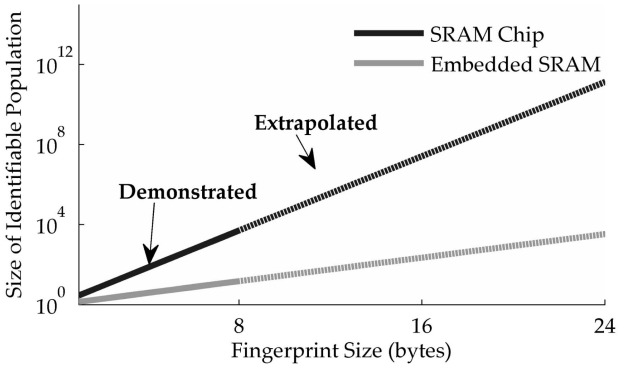

Fig. 7. The size of population in which members can be uniquely identified as a function of the size of the fingerprint, for both the SRAM chip and embedded SRAM. The solid lines are demonstrated through experiment, while the dashed lines are extrapolated.

Similarly, each 64-bit embedded SRAM fingerprint is shown to provide at least 3.9 bits of ID, or 0.06 bits of ID per cell.

Based on the amount of identity provided per cell, the identifying ability of larger fingerprints is extrapolated. For example, a 16-byte fingerprint from the SRAM chip (providing 0.192 bits of ID per cell) would provide 24.6 bits of ID, sufficient for identification among a population of $2^{24.6}$, over 26 million. This analysis is generalized to different size fingerprints of both platforms in Fig. 7.

4.3 Comparison to Existing Work

With regard to the mechanism for generating ID based on threshold voltage mismatch in cross-coupled devices, the FERNS method is similar to, and inspired by, the recent ISSCC 2007 design of Su et al. [17]. In this related work, a cross-coupled NOR cell is used to generate the ID. When the control signal is set low, the cross-coupled devices are isolated from the supply and both state nodes are pulled low; the circuit in this state is analogous to the cross-coupled inverters in an unpowered SRAM cell. To obtain the ID, the cross-coupled devices are connected to the supply rail, causing the cell to stabilize to one of two stable states; the choice of stable state represents the identity of the cell. This behavior is analogous to the powering-up of an SRAM cell.

The design of Su et al. gives excellent performance, but it comes at a high area cost; we present a case that this cost is excessive. One reason for the excellent performance of this design is the use of analog layout techniques to minimize the impact of noise and correlated process effects. These layout techniques minimize the number of unstable cells and maximize the fractional Hamming distance across chips but also result in a low transistor density; the area of each ID cell is 40 μm^2, and additional area is consumed by surrounding the ID cells with dummy cells to ensure isolation from any potential noise sources. Contrary to this specialized and sparse layout, the large production quantities of conventional SRAM cells justify a density-optimized layout, with cell areas of just 3 μm^2 at the same 0.13-μm technology node [32].

With 13 SRAM cells consuming less total area than each ID cell from Su's design, comparing their per-cell identifying ability does not give a true measure of how efficiently each design is using chip area. Instead, the designs are compared using a cost metric of area per ID bit, calculated as area per cell divided by the amount of usable identity generated by each cell (9). This metric is applied conservatively to FERNS by basing the amount of identity contained in each SRAM cell on the lower bound of what has been demonstrated (7). The identifying ability of the design of Su et al. is overestimated, by assuming that each cell produces a perfect bit of identity.

$$Area\ per\ ID\ bit = \frac{Area/cell}{ID_{bits}/cell}. \tag{9}$$

According to this metric of area per ID bit, SRAM fingerprints provide identification with comparable efficiency to the work of Su et al. (Table 1). However, there are some notable differences between how the two works can be applied. The FERNS method has the advantage that the area used to generate the identifying fingerprint is not dedicated to the task but is instead general purpose SRAM. A drawback to the FERNS approach is that the identifier is only generated at power-up and is destroyed once data are written to the SRAM. The fingerprint can only be regenerated by cycling the power to the SRAM.

5 FERNS for True Random Number Generation

Experiments show that 512 bytes of latent fingerprint can be used to create a 128-bit true random number. As explained in Section 3, the neutral-skewed cells in the SRAM can power-up to either state in the presence of noise. This causes latent fingerprints to be randomized (Fig. 8). In essence, the neutral-skewed SRAM cells function as tiny, imprecise, six-transistor TRNG circuits scattered across the SRAM array, generating and storing random bits at

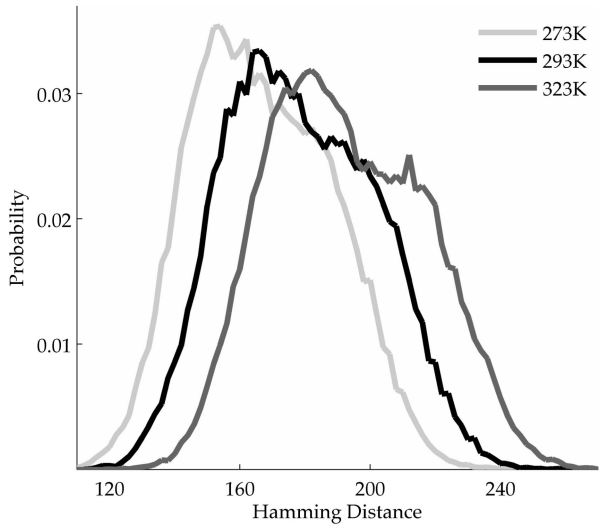

Fig. 8. Distribution of observed pairwise Hamming distances between 45,900 pairings of 512-byte latent fingerprints, repeated at three temperatures. Each pairing represents two power-ups of the same logical SRAM device; 1,024 logical SRAM devices were used. The increase in Hamming distances with temperature indicates increasing randomness. For comparison, note that a pairing of 128-bit random numbers would have an expected Hamming distance of only 64 bits.

power-up. This section deals with how to quantify, extract, and evaluate the randomness for use in FERNS.

Note that the experimental TRNG results are from the SRAM chip and not the embedded SRAM, which has only 256 bytes of SRAM. The Hamming distance between latent and known fingerprints generated by the same device is smaller for SRAM chip design, indicating less randomness and implying that the conclusions drawn from the SRAM chip would likely also apply to the embedded SRAM design. Nonetheless, the amount of randomness contained in any SRAM design should be quantified before it is used for generating random numbers.

5.1 Entropy Extraction

To extract the randomness from the latent fingerprints, privacy amplification is employed. In general terms, privacy amplification techniques are used to extract a secret from a body of information about which an adversary has partial knowledge. Mapping privacy amplification to the domain of this work, the extracted secret is the random number, the body of information is the latent SRAM fingerprint generated at power-up, and the partial knowledge of the adversary is knowledge of the tendency of each SRAM cell.

5.1.1 Guessing Probability and Min-Entropy

To apply privacy amplification, bounds are first established on the information that an adversary can possess about an unobserved latent fingerprint, using the metrics of guessing probability and min-entropy [33]. In trying to predict the latent fingerprint, the best possible guess of any adversary is the most likely power-up state of the SRAM. The probability that the SRAM will generate this particular latent fingerprint is the guessing probability of the system and gives an upper bound on the capabilities of any adversary.

To directly measure the guessing probability of the power-up state of the SRAM is prohibitively expensive, requiring on the order of 2^{128} samples. Instead, it is estimated based on the guessing probability of each byte and the assumption that all 512 bytes are independent. The guessing probability of each byte is found by observing the most likely outcome across 100 trials:

$$X = \{B_1, B_2, \ldots, B_{512}\}, \tag{10}$$

$$\gamma(B_N) = \max\Big\{P[B_N = b] : b \in \{0,1\}^8\Big\}. \tag{11}$$

Under the assumption that the bytes are independent, the guessing probability of the 512-byte latent fingerprint is the product of the guessing probability of the constituent bytes:

$$\gamma(X) = \prod_{n=1}^{512} \gamma(B_N). \tag{12}$$

Supporting the assumption of bytewise independence, the guessing probability was found not to change significantly when considering blocks larger and smaller than the nominal size of 1 byte. Min-entropy measures the entropy contained in the most probable power-up state of the SRAM [33]:

$$H_\infty(X) = \log_2\left(\frac{1}{\gamma(X)}\right). \tag{13}$$

Min-entropy thus provides a lower bound on the amount of randomness contained in the power-up state of the SRAM. It is found that min-entropy of SRAM power-up state varies with temperature. To tolerate this, and possible inaccuracies in our estimation of min-entropy, we design conservatively, with 128 random bits generated from a source estimated to contain 189 bits of min-entropy in the worst case (Table 2).

TABLE 2
The Observed Min-Entropy and Associated Guessing Probability for Each Temperature Used in Experiment

Temp(K)	**Min-Entropy** $(bits)$	**Guessing Probability**
273	189.2	$2^{-189.2}$
293	202.3	$2^{-202.3}$
323	218.7	$2^{-218.7}$

5.1.2 PH Universal Hashing Function

Universal hash functions are cryptographic hash functions capable of privacy amplification [34]. The low collision probability of universal hash functions allows them to be used for randomness extraction [35]. Extraction in FERNS is performed by hashing a 512-byte fingerprint into 128 bits using the PH universal hash function of Yüksel et al. [36], with each block of message and key comprised of the power-up state of 64 bits of SRAM:

$$PH_K(M) = \sum_{i=1}^{16}(m_{2i-1} + k_{2i-1})(m_{2i} + k_{2i}). \tag{14}$$

$$M = (m_1, \ldots, m_{32}) \quad K = (k_1, \ldots, k_{32}). \tag{15}$$

$$m_i, k_i \in GF(2). \tag{16}$$

PH is designed for low gate count and low-power hardware implementation with all operations performed over GF(2), so that addition and multiplication reduce to a series of shift and XOR operations.

5.1.3 Statistical Testing of Extracted Random Bits

While min-entropy is intended as the primary assurance of randomness for the extracted bits, these bits are also tested using the runs, approximate entropy, and block frequency tests from the NIST suite [37]. Over 52 million bits of power-up state are hashed into 12,800 128-bit random numbers for testing. As a compromise between testing large blocks of random bits and testing many blocks of random bits, the tests are performed on 1,280 blocks of 1,280 bits each, with each block being a concatenation of 10 128-bit random numbers. The random numbers pass each of the tests (Table 3), further supporting the feasibility of extracting statistically random numbers from the power-up state of ordinary commercial SRAM chips using a simple low-cost entropy extracting code.

TABLE 3
Output from NIST Tests for Runs, Approximate Entropy, and Block Frequency, Applied to the Random Numbers Produced by FERNS

C1	C2	C3	C4	C5	C6	C7	C8	C9	C10	P VAL	PROP	TEST
134	131	129	126	129	108	131	119	139	134	0.7931	0.9922	runs
139	122	124	132	138	124	122	120	126	133	0.9467	0.9945	apen
119	124	147	121	125	116	147	134	130	117	0.4159	0.9898	block-frequency

The uniform distribution across columns c_1 through c_{10} indicates a uniform distribution for the frequency of various P values. The 11th column indicates the P value obtained via a chi-square test. The 12th column indicates the proportion of binary sequences that passed testing. The random numbers generated by FERNS pass each test.

5.2 Comparison to Existing Work

With regard to the mechanism for generating entropy, the FERNS method is compared to, and contrasted against, the recent ISSCC 2007 TRNG design of Tokunaga et al. [30]. Both designs create random numbers using metastable cross-coupled CMOS devices. In Tokunaga's design, a single cross-coupled cell is biased precisely to the metastable point and then allowed to stabilize, with the stable state then determined by noise. Because the metastable bias point is not static, dynamic control and feedback are used to set the cell to the metastable point. A delay test is used to judge the metastability; the probability that the bias point is truly metastable increases with the time required to resolve the metastability. A notable benefit of this approach is that the bits produced are assured to be determined by thermal noise, but a drawback is that having a precise timer and control system consumes power and area.

The FERNS method of extracting randomness from SRAM is akin to using a very imprecise version of Tokunaga's design. In FERNS, massive redundancy compensates for the imprecision, with the randomness scattered throughout the SRAM (Fig. 9). No feedback or control is required, because there is no need to precisely bias a single cross-coupled cell to perfect metastability. Instead, FERNS relies on the large number of cells to ensure that *some* cells will be influenced by noise when the chip is powered-up, without giving concern to which cells are generating randomness. In fact, when the chip is powered-up in different conditions, different cells become random (see Section 6.2), demonstrating a potential resiliency against external influences.

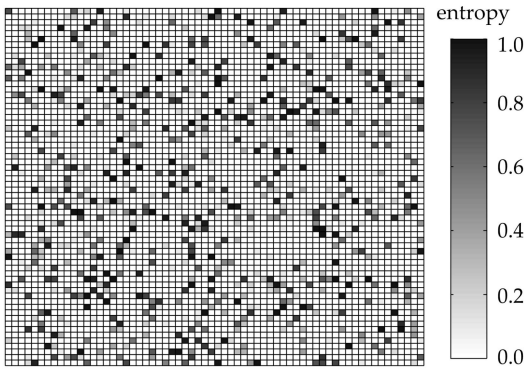

Fig. 9. SRAM cells with unpredictable power-up states, shaded dark, are scattered throughout a 512-byte section—the quantity used to create a single 128-bit random number. The entropy of each cell is determined from 100 power-ups at 293 K.

5.2.1 Estimated Area Costs

The tradeoff of precision against redundancy has implications on the area cost. In Tokunaga's circuit, the majority of silicon area is consumed by the control logic (Table 4). Because FERNS is using 512 bytes of SRAM, FERNS requires more area for its metastable circuitry. However, the PH universal hashing function, requiring only 557 cells, is roughly a quarter of the size of the counter and charge injection circuitry used in Tokunaga's circuit.

5.2.2 Fixed versus Unlimited Entropy Generation

The primary limitation of the FERNS TRNG is that entropy is only generated during power-up. This contrasts poorly against the unbounded entropy generation potential of any dedicated TRNG circuit. If random numbers will be needed during a time other than power-up, the random numbers must be extracted and stored from power-up until use. For this reason, the FERNS method is best suited to applications that are intermittently powered and do not require large quantities of random numbers.

5.2.3 Custom versus General Purpose Circuitry

The preceding paragraphs have shown that FERNS can generate random numbers in comparable area to a dedicated circuit but is greatly limited in the amount of randomness it can generate on account of only being able to generate entropy at power-up; not a very compelling case for FERNS TRNG thus far. The strength of the FERNS method is the ability to generate true random numbers without any dedicated circuitry. Both the hash function and the SRAM itself are common parts that can be reused. In embedded applications such as RFID or smart cards, a cryptographic hash function is likely to be preexisting for security functionality. In a microcontroller, the PH hashing can be performed using only XOR and bitshift operations that are found as primitives in nearly all instruction set architectures. By offering TRNG using commonly available circuitry, the FERNS method may enable TRNG in some applications that were previously incapable of it.

TABLE 4
Comparing the Estimated Area of FERNS with that of Related Work, Based on 0.13-μm Technology

Tokunaga et al. [30]		FERNS	
Function	**Area**(μm^2)	**Function**	**Area**(μm^2)
Metastable Module	6,000	SRAM Array	12,300
Control	29,900	PH Hashing	7,400
Total	35,900	Total	19,700

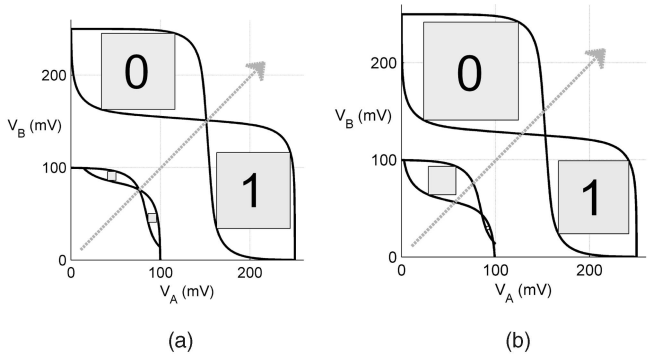

Fig. 10. VTCs obtained from SPICE simulation of a skewed and neutral SRAM cell at 100- and 250-mV supply voltages. (a) SNMs of unskewed cell. (b) SNMs of 0-skewed cell.

6 Robustness to Environmental Factors

The viability of the FERNS method depends on how sensitive the fingerprint identity and TRNG are to the environments where the circuit will be used. This section explores the potential influence of supply voltage, ambient temperature, and negative bias temperature instability (NBTI) on power-up SRAM state.

6.1 Supply Voltage

The ability of an SRAM cell to hold state depends on noise, the process variation of the cell, and the applied supply voltage. Low supply voltage leaves a cell susceptible to noise-induced state changes, while higher voltage makes a cell stable and immune to noise. The minimum supply voltage at which an SRAM cell is able to tolerate "reasonable" noise without changing state varies from cell to cell, is determined by variation, and typically falls in the range of 100 to 300 mV [38]. During power-up, it is assumed that the supply voltage begins at 0 V, where all cells can be influenced by noise, and increases to a nominal operating voltage well above 300 mV, where all cells are stable in the 0 or 1 state and not influenced by noise. The randomness and identity in power-up SRAM state is thus determined by cell behaviors at low supply voltages.

Static Noise Margin (SNM) is the metric for quantifying the noise immunity of an SRAM cell. The SNM of a cell at a given supply voltage is defined as the maximum noise voltage that can be tolerated before changing state [39]. SNM is measured as the shortest side of the largest box that can be placed inside of the eye of the Voltage Transfer Curves (VTCs) of the cross-coupled inverters that comprise the cell [40], [41]. A noise-immune cell has two large eyes between the inverter VTCs. SNM is greatly diminished at low supply voltages (Fig. 10). In cells that are not skewed by variation, low supply voltage causes the SNM of each state to be equally small (Fig. 10a). However, in highly skewed cells, low supply voltage can reduce the SNM of one state to 0 V, indicating the existence of a single noise-immune state (Fig. 10b).

6.1.1 Relevance to FERNS Method

By controlling how quickly the supply voltage ramps up, it may be possible to influence the power-up state to be less random. Consider the case of the skewed SRAM cell described by the VTCs in Fig. 10b. If the supply voltage is held at 100 mV during power-up, even the slightest noise will induce a transition to the 0 state favored by this cell. The probability of this transition increases with the amount of time that the supply is held at 100 mV. Note that there is nothing unique about this particular cell or supply voltage; any skewed cell will have some voltage at which a transition to the favored state is inevitable, given sufficient time. By increasing the supply voltage very slowly, one could likely create an exceptionally identifying power-up fingerprint with an increased number of cells powering-up to their favored state. If an adversary could control the supply voltage in this way, he might be able to reduce the entropy of the random numbers extracted from the SRAM power-up fingerprints.

TABLE 5
Estimated Thermal Noise, Threshold Voltages, and Mobilities at Experiment Temperatures

$T(K)$	$\sigma^2_{noise}(\mu V)$	$V_{TH}(mV)$ P	$V_{TH}(mV)$ N	$\mu(cm^2/Vs)$ P	$\mu(cm^2/Vs)$ N
273	17.5	311	474	555	1727
293	18.8	288	452	482	1499
323	20.7	254	419	451	1402

6.2 Impact of Temperature

While the temperature of high-performance VLSI circuits can exceed 400 K, the range of temperatures relevant to FERNS is modest by comparison because SRAM fingerprints are generated at power-up before any self-heating has occurred. To represent extreme ambient temperatures that an SRAM might encounter at power-up, experiments are performed at 273 K (freezing point of water), 293 K (room temperature), and 323 K (among the hottest recorded temperatures on earth).

The impact of temperature on MOSFET devices is well studied in literature. An increase in temperature decreases device threshold voltages:

$$V_{th}(T) = V_{th}(T_o) - \kappa \Delta T, \tag{17}$$

while also decreasing the electron and hole mobilities [42]:

$$\mu(T) = \mu_0 \left(\frac{T}{300}\right)^{\alpha}. \tag{18}$$

These two trends may counteract each other during power-up, since a lowered threshold will increase subthreshold current, while reduced mobility will decrease subthreshold current. Additionally, an increase in temperature increases the magnitude of thermal noise

$$\sigma^2_{NOISE}(T) = \frac{2K_B T}{C}, \tag{19}$$

which could lead to a more random power-up state. The estimated thermal noise, threshold voltages, and carrier mobilities for each temperature are given in Table 5; threshold voltages are obtained from 0.18-μm BSIM3 models [43], thermal noise is calculated based on 0.430-fF node capacitances, and mobilities are calculated using values of -2 for α and 480 and 1,350 $\mathrm{cm}^2/\mathrm{Vs}$ for μ_{0p} and μ_{0n}, respectively. The influence of these changing MOSFET characteristics on

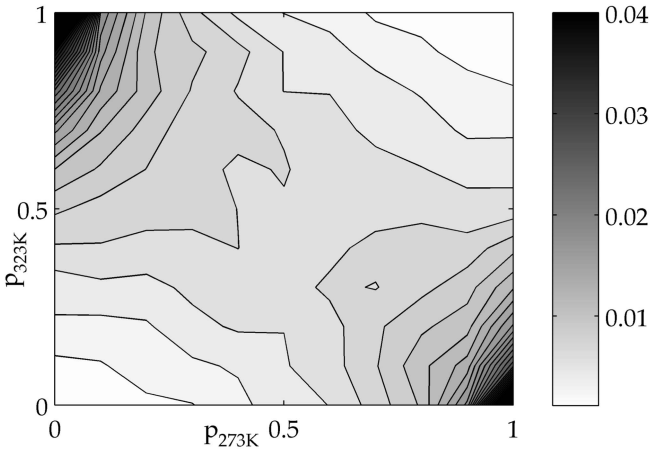

Fig. 11. This contour shows the probability distribution at 273 and 323 K, of all cells that are neutral at 293 K. Note that the probability exceeds 0.04 at the highest points; these peaks are omitted to show the rest of the distribution with greater detail. See Section 6.2.1 for discussion.

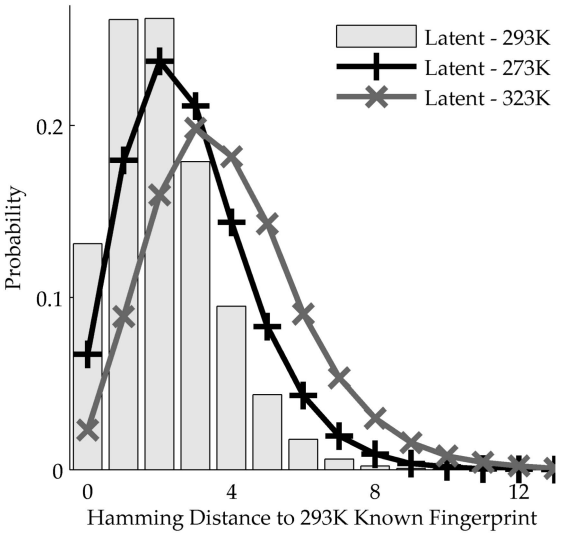

Fig. 12. Matching the nominal known fingerprints against latent fingerprints taken at different temperatures shows that fingerprint IDs change only slightly with temperature.

SRAM power-up state is difficult to model because power-up state is not determined directly by the MOSFET devices but instead by the relative strengths of cross-coupled devices that are similarly impacted by temperature.

6.2.1 Observed Tendencies of Neutral Cells

Determining how the skew of an SRAM cell changes with temperature is challenging, as the only measurement that can be made is p, the probability of a given cell initializing to 1 (2). The power-up tendencies of neutral-skewed cells can provide some insights on the influence of temperature. On a 512-Kbyte SRAM chip under nominal conditions, over 30,000 cells are found to be neutral (p_{293} is 0.5). The same chip is powered-up 10 times at each of the other temperatures, and the tendencies of these neutral cells are observed; each one can then be classified as a triple of p values $(p_{273}, p_{293}, p_{323})$. The contour plot of Fig. 11 shows the distribution of observed triples; note that p_{293} does not appear explicitly, since all cells contributing to the distribution have 0.5 for p_{293}. The data in this plot leads to three insights regarding how the power-up tendencies of cells shift with temperature:

1. **The skew of a cell can change with temperature.** Cells that are neutral at 293 K are typically not also neutral at other temperatures. Instead, the majority of these cells become 0-skewed or 1-skewed when the temperature is changed. This is indicated by the relatively low probabilities around $(0.5_{273}, 0.5_{293}, 0.5_{323})$ and the significantly higher probabilities occurring at $(0_{273}, 0.5_{293}, 1_{323})$ and $(1_{273}, 0.5_{293}, 0_{323})$.
2. **Skew shift is monotonic with respect to temperature.** If an increase in temperature makes a neutral cell become 1-skewed, then decreasing the temperature will typically make that same cell 0-skewed. This trend is observed in the high probabilities at $(0_{273}, 0.5_{293}, 1_{323})$ and $(1_{273}, 0.5_{293}, 0_{323})$ compared to the lower probabilities at $(1_{273}, 0.5_{293}, 1_{323})$ and $(0_{273}, 0.5_{293}, 0_{323})$.
3. **The direction of skew shift differs from cell to cell.** Although individual cell tendencies do change monotonically with temperature, they do not all shift in the same direction. Of the cells that are neutral at 293 K, some become 1-skewed at higher temperatures and 0-skewed at lower temperatures, while the opposite trend is seen in other cells. This is observed in the high probabilities occurring at both $(0_{273}, 0.5_{293}, 1_{323})$ and $(1_{273}, 0.5_{293}, 0_{323})$.

6.2.2 Relevance to FERNS Method

Temperature is only a minor concern for the quality of identification and random numbers produced in FERNS. Although the 50-mV threshold shift across the range of experiment temperatures is approximately twice the standard deviation of the device thresholds, the ID in FERNS only depends on the *relative* strengths of the two cross-coupled inverters (see Section 3.1). The common-mode effects of temperature do not significantly favor one state over the other. Experiments show that Hamming distances between known fingerprints generated at 293 K and latent fingerprints taken at 273 or 323 K are only slightly larger than those obtained when both latent and known fingerprints are generated at 293 K (Fig. 12).

The min-entropy of SRAM fingerprints increases with temperature (Table 2). However, without being able to properly attribute this to an increase in thermal noise, it is unknown whether an adversary could use temperature to influence the quality of the TRNG. With this in mind, the TRNG is designed conservatively; in the worst case (273 K), an estimated 189 bits of min-entropy are used to create 128 random bits. Larger SRAM fingerprints can be used if a greater assurance of entropy is desired.

6.3 Negative Bias Temperature Instability

Prior work in secure hardware has shown that storing data in SRAM cells for long periods of time can cause burn-in, allowing the data to be reconstructed long after it was stored [44]. A modern version of burn-in to consider is NBTI. NBTI is a phenomenon by which deep submicron MOSFET threshold voltages increase over time due to applied stress

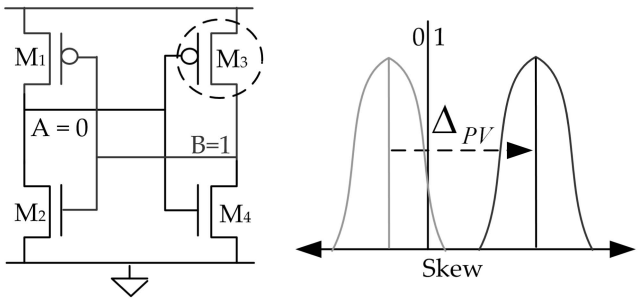

Fig. 13. NBTI raises the threshold of stressed PMOS device M_3 and skews the power-up state of the cell away from the 0 state $(AB = 01)$ that was causing the stress.

conditions of high temperature and a vertical electric field caused by the voltage at the MOSFET gate terminal. This electric field creates the inversion channel that allows the MOSFET to conduct current and is present whenever a device is turned on. The NBTI-induced increase in threshold voltage grows with the amount of time that the stress conditions are applied [45]. Once the stress is removed, devices begin to recover; in cases where only a high gate voltage is applied without high temperature, recovery can reach 100 percent [46]. While NBTI can impact both PMOS and NMOS devices, PMOS NBTI dominates [47].

6.3.1 Analysis of NBTI Impact

NBTI causes the skew of each SRAM cell to shift away from the value previously stored by the cell. Consider a slightly 0-skewed SRAM cell that stores a 0 $(AB = 01)$, as depicted in Fig. 13. Device M_3 experiences NBTI stress conditions while the cell stores the 0 and, consequently, has an increased threshold voltage afterward. The next time this cell is powered-up, the higher threshold voltage of M_3 (neglecting recovery) causes it to turn on more slowly than normal, making the cell less likely to power-up to 0 $(AB = 01)$ than it was before NBTI stress, and more likely to power-up to the opposing 1 state.

6.3.2 NBTI Burn-In Experiments

The conclusion that NBTI causes a cell storing a given value to favor the opposite value in the next power-up is supported by four NBTI burn-in experiments. Each experiment is performed sequentially on the same 512-Kbyte SRAM chip and takes the following form:

1. Power-up SRAM at 313 K and write 0 into all cells;
2. Maintain power and temperature, burning-in the 0 state for specified stress time;
3. Power down SRAM and remain powered-down for specified recovery time;
4. Power-up SRAM again and read out state to determine Hamming weight.

Three of the experiments use a burn-in of 1.7×10^5 seconds (two days) with varied recovery times, and the fourth experiment uses a longer burn-in time of 8.6×10^5 seconds (10 days). The Hamming weights from each are compared to a set of previously obtained baseline measurements taken at room temperature under nominal conditions. In all four experiments, the average Hamming weight of the SRAM cells

TABLE 6
Observed Average Hamming Weights before and after NBTI Stress

Stress Time(s)	Recovery Time(s)	Hamming Weight
$8.6 * 10^5$	20	0.7749
$1.7 * 10^5$	20	0.7626
$1.7 * 10^5$	180	0.7561
$1.7 * 10^5$	420	0.7527
Baseline - 1		0.7508
Baseline - 2		0.7510
Baseline - 3		0.7508
Baseline - 4		0.7507

increased significantly after burning-in the 0 state, consistent with prediction. Substantial NBTI recovery is observed, but full recovery does not occur within 420 seconds (Table 6).

6.3.3 Relevance to FERNS Method

Normal usage patterns of intermittently powered devices operating at low temperatures should prevent incidental NBTI from being a significant concern. However, if used maliciously under atypical conditions, NBTI could be a threat to FERNS because it provides a way to skew each cell toward a chosen power-up state. This is illustrated by contrasting the impact of NBTI against the impact of varying SRAM temperature (Fig. 14), when both are applied to the same 512-Kbyte SRAM chip. All cells are first classified according to their p values (2) under nominal conditions. When the chip is then powered-up at one temperature, the expected value $(E(p))$ of the power-up state of all cells in each p classification is calculated; this is

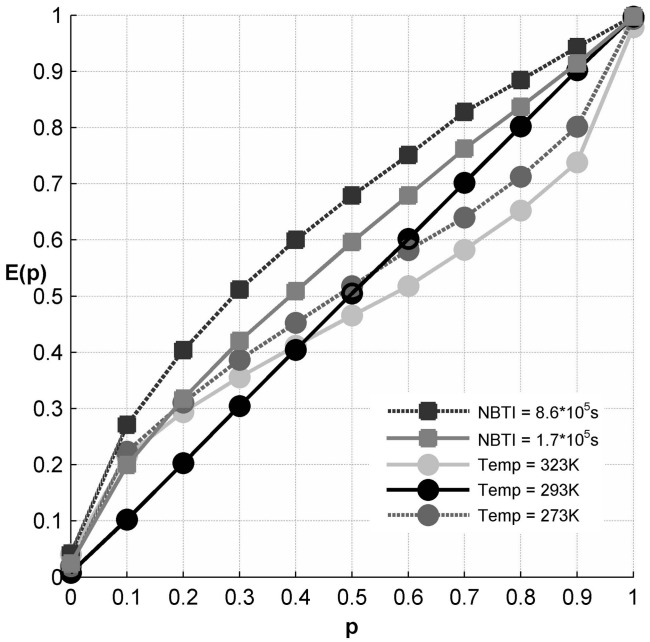

Fig. 14. The expected value of the power-up state of a cell at varied temperature, or after NBTI stress, is plotted as a function of the probability p of the same cells powering-up to 1 under nominal conditions. Using NBTI to burn-in 0 values causes cells of all nominal probabilities to be slightly more likely to power-up to the 1 state, while varying temperature induces random shifts, causing the expected value of cells of all nominal probabilities to tend toward 0.5.

repeated for temperatures 273, 293, and 323 K, and for NBTI burn-in durations of 1.7×10^5 and 8.6×10^5 seconds (both with 20-second recovery time). The NBTI burn-in of the 0 state skews cells across all nominal probabilities toward the 1 state; for example, among all cells that have a 50 percent probability of powering-up to 1 under nominal conditions, 59 percent power-up to 1 after the moderate NBTI burn-in, and 68 percent power-up to 1 after the longer burn-in. Across all nominal tendencies, NBTI burn-in of the 0 state causes cells to become more likely to power-up to the 1 state. This predictable influence of NBTI stands in contrast to the unpredictable skew shifts induced by increasing or decreasing temperature, which overall cause the expected values to trend toward 0.5 across all nominal p skews.

7 Conclusions and Future Work

In this paper, we have presented the FERNS method for using SRAM physical fingerprints to identify circuits and generate true random numbers. We show that the power-up state of just 8 bytes of a commercially available SRAM is sufficient for identification among a population of 5,120 instances and that 512 bytes of the same SRAM produce enough randomness to generate 128-bit numbers capable of passing statistical tests for randomness. The identity in the SRAM fingerprint comes from the inherent threshold voltage mismatch of MOSFET devices, and the randomness results from noise impacting SRAM cells that do not have significant mismatch.

The strength of the FERNS method is that no dedicated circuits are required. Aside from the SRAM used to generate the fingerprints, the randomness extraction requires only a hash function or simple processing core capable of bitshift and bitwise XOR operations. Given the ubiquity of these enabling parts, we believe that FERNS can find use across the spectrum of integrated circuit applications, ranging from low cost passively powered RFID tags and smart cards up through embedded caches on high-end devices.

Future work on FERNS will explore implementation of a derivative design and the effectiveness of possible attacks discussed in this paper.

Acknowledgments

This material is based upon work supported by the US National Science Foundation under Grant 0627529. The authors would like to thank Thomas Heydt-Benjamin for his discussion on potential applications for SRAM physical fingerprints, Intel Research and Joshua R. Smith for providing and supporting the WISP platforms, and Adam Stubblefield for reviewing an early manuscript and providing feedback that has helped guide the development of this work. The authors would also like to thank the anonymous reviewers for their insightful and constructive comments on this work.

References

[1] I. Goldberg and D. Wagner, "Randomness and the Netscape Browser," *Dr. Dobbs J.*, pp. 66-70, 1996.

[2] T.S. Heydt-Benjamin, D.V. Bailey, K. Fu, A. Juels, and T. O'Hare, "Vulnerabilities in First-Generation RFID-Enabled Credit Cards," *Proc. 11th Int'l Conf. Financial Cryptography and Data Security (FC '07)*, http://prisms.cs.umass.edu/~kevinfu/papers/RFID-CC-manuscript.pdf, Feb. 2007.

[3] D. Halperin, T.S. Heydt-Benjamin, B. Ransford, S.S. Clark, B. Defend, W. Morgan, K. Fu, T. Kohno, and W.H. Maisel, "Pacemakers and Implantable Cardiac Defibrillators: Software Radio Attacks and Zero-Power Defenses," *Proc. 29th Ann. IEEE Symp. Security and Privacy (S&P '08)*, May 2008.

[4] D.E. Holcomb, W.P. Burleson, and K. Fu, "Initial SRAM State as a Fingerprint and Source of True Random Numbers for RFID Tags," *Proc. Conf. Radio Frequency Identification Security (RFID '07)*, July 2007.

[5] *IS61LV25616AL—256K × 16 High Speed Asynchronous CMOS Static RAM with 3.3 V Supply*, Integrated Silicon Solution, http://www.issi.com/pdf/61LV25616AL.pdf, Feb. 2006.

[6] *Altera's Development and Education Board*, Altera, http://www.altera.com/education/univ/materials/boards/unv-de2-board.html, 2007.

[7] J.R. Smith, A. Sample, P. Powledge, S. Roy, and A. Mamishev, "A Wirelessly-Powered Platform for Sensing and Computation," *Proc. Eighth Int'l Conf. Ubiquitous Computing (UbiComp '06)*, pp. 495-506, 2006.

[8] A.P. Sample, D.J. Yeager, P.S. Powledge, and J.R. Smith, "Design of a Passively-Powered, Programmable Platform for UHF RFID Systems," *Proc. IEEE Int'l Conf. Radio Frequency Identification (RFID '07)*, pp. 149-156, Mar. 2007.

[9] A.P. Sample, D.J. Yeager, P.S. Powledge, A.V. Mamishev, and J.R. Smith, "Design of an RFID-Based Battery-Free Programmable Sensing Platform," *IEEE Trans. Instrumentation and Measurement*, vol. 57, no. 11, pp. 2608-2615, Nov. 2008.

[10] D.C. Ranasinghe, D. Lim, P.H. Cole, and S. Devadas, "White Paper: A Low Cost Solution to Authentication in Passive RFID Systems," Technical Report WP-HARDWARE-029, Auto-ID Labs, The Univ. of Adelaide, Sept. 2006.

[11] *MSP430x11x2 MSP430x12x2 Mixed Signal Microcontroller*, Texas Instruments, http://focus.ti.com/lit/ds/symlink/msp430f1232.pdf, Aug. 2004.

[12] *Nonvolatile Semiconductor Memory Technology: A Comprehensive Guide to Understanding and Using NVSM Devices*, W.D. Brown and J.E. Brewer, eds., Wiley-IEEE Press, 1997.

[13] P. Friedberg, W. Cheung, and C. Spanos, "Spatial Variability of Critical Dimensions," *Proc. VLSI/ULSI Multilevel Interconnection Conf. XXII*, pp. 539-546, 2005.

[14] X. Tang, V.K. De, and J.D. Meindl, "Intrinsic MOSFET Parameter Fluctuations Due to Random Dopant Placement," *IEEE Trans. Very Large Scale Integration (VLSI) Systems*, pp. 369-376, Dec. 1997.

[15] "Design," *Int'l Technology Roadmap for Semiconductors*, ITRS, Update, 2006.

[16] K. Lofstrom, W. Daasch, and D. Taylor, "IC Identification Circuit Using Device Mismatch," *Proc. IEEE Int'l Solid-State Circuits Conf. (ISSCC '00)*, Digest of Technical Papers, pp. 372-373, 2000.

[17] Y. Su, J. Holleman, and B. Otis, "A 1.6 pJ/bit 96% Stable Chip ID Generating Circuit Using Process Variations," *Proc. IEEE Int'l Solid-State Circuits Conf. (ISSCC '07)*, Digest of Technical Papers, 2007.

[18] P. Layman, S. Chaudhry, J.G. Norman, and J.R. Thomson, *Electronic Fingerprinting of Semiconductor Integrated Circuits*, Patent 6,738,294, Sept. 2002.

[19] R.S. Pappu, B. Recht, J. Taylor, and N. Gershenfeld, "Physical One-Way Functions," *Science*, vol. 297, no. 6, pp. 2026-2030, http://web.media.mit.edu/~brecht/papers/02.PapEA.powf.pdf, 2002.

[20] P. Tuyls, G.-J. Schrijen, B. Skoric, J. van Geloven, N. Verhaegh, and R. Wolters, "Read-Proof Hardware from Protective Coatings," *Proc. Eighth Int'l Workshop Cryptographic Hardware and Embedded Systems (CHES '06)*, vol. 4249, pp. 369-383, Oct. 2006.

[21] G. DeJean and D. Kirovski, "RF-DNA: Radio-Frequency Certificates of Authenticity," *Proc. Ninth Int'l Workshop Cryptographic Hardware and Embedded Systems (CHES '07)*, pp. 346-363, 2007.

[22] B. Gassend, D. Clarke, M. van Dijk, and S. Devadas, "Silicon Physical Random Functions," *Proc. Ninth ACM Conf. Computer and Comm. Security (CCS '02)*, pp. 372-373, 2002.

[23] G. Suh, C. O'Donnell, I. Sachdev, and S. Devadas, "Design and Implementation of the AEGIS Single-Chip Secure Processor Using Physical Random Functions," *Proc. 32nd Int'l Symp. Computer Architecture (ISCA '05)*, pp. 25-36, 2005.

[24] J. Guajardo, S.S. Kumar, G.-J. Schrijen, and P. Tuyls, "FPGA Intrinsic PUFs and Their Use for IP Protection," *Proc. Workshop Cryptographic Hardware and Embedded Security*, pp. 63-80, Sept. 2007.

[25] J. Guajardo, S.S. Kumar, G.-J. Schrijen, and P. Tuyls, "Physical Unclonable Functions and Public-Key Crypto for FPGA IP Protection," *Proc. Int'l Conf. Field Programmable Logic and Applications (FPL '07),* pp. 189-195, Aug. 2007.

[26] H. Nyquist, "Thermal Agitation of Electric Charge in Conductors," *Physical Rev.,* vol. 32, no. 110, 1928.

[27] J. Johnson, "Thermal Agitation of Electricity in Conductors," *Physical Rev.,* vol. 32, no. 97, 1928.

[28] B. Sunar, W.J. Martin, and D.R. Stinson, "A Provably Secure True Random Number Generator with Built-In Tolerance to Active Attacks," *IEEE Trans. Computers,* vol. 58, pp. 109-119, Jan. 2007.

[29] D.J. Kinnimet and E. Chester, "Design of an On-Chip Random Number Generator Using Metastability," *Proc. 28th European Solid-State Circuits Conf. (ESSCIRC '02),* pp. 595-598, 2002.

[30] C. Tokunaga, D. Blaauw, and T. Mudge, "A True Random Number Generator with a Metastability-Based Quality Control," *Proc. IEEE Int'l Solid-State Circuits Conf. (ISSCC '07),* Digest of Technical Papers, 2007.

[31] J.M. Rabaey, A. Chandrakasan, and B. Nikolic, *Digital Integrated Circuits: A Design Perspective,* second ed. Prentice Hall, 2003.

[32] K. Osada, Y. Saitoh, E. Ibe, and K. Ishibashi, "16.7-fA/cell Tunnel-Leakage-Suppressed 16-Mb SRAM for Handling Cosmic-Ray-Induced Multierrors," *IEEE J. Solid-State Circuits,* vol. 38, no. 11, pp. 1952-1957, Nov. 2003.

[33] V. Shoup, *A Computational Introduction to Number Theory and Algebra.* Cambridge Univ. Press, 2005.

[34] L. Carter and M.N. Wegman, "Universal Classes of Hash Functions," *J. Computer and System Sciences,* vol. 18, no. 2, pp. 143-154, 1979.

[35] N. Nisan and A. Ta-Shma, "Extracting Randomness: A Survey and New Constructions," *J. Computer and System Sciences,* vol. 58, no. 1, pp. 148-173, 1999.

[36] K. Yüksel, J.P. Kaps, and B. Sunar, "Universal Hash Functions for Emerging Ultra-Low-Power Networks," *Proc. Comm. Networks and Distributed Systems Modeling and Simulation Conf. (CNDS '04),* Jan. 2004.

[37] Rukhin et al., *A Statistical Test Suite for Random and Pseudorandom Number Generators for Cryptographic Applications,* NIST Special Publication 800-22 (revised May 2002), 2002.

[38] H. Qin, Y. Cao, D. Markovic, A. Vladimirescu, and J. Rabaey, "SRAM Leakage Suppression by Minimizing Standby Supply Voltage," *Proc. Fifth Int'l Symp. Quality Electronic Design (ISQED '04),* pp. 55-60, 2004.

[39] E. Seevinck, F. List, and J. Lohstroh, "Static-Noise Margin Analysis of MOS SRAM Cells," *IEEE J. Solid-State Circuits,* vol. 22, no. 5, pp. 748-754, Oct. 1987.

[40] K. Agarwal and S. Nassif, "Statistical Analysis of SRAM Cell Stability," *Proc. 43rd ACM/IEEE Design Automation Conf. (DAC '06),* pp. 57-62, July 2006.

[41] A. Bhavnagarwala, X. Tang, and J. Meindl, "The Impact of Intrinsic Device Fluctuations on CMOS SRAM Cell Stability," *IEEE J. Solid-State Circuits,* vol. 36, no. 4, pp. 658-665, Apr. 2001.

[42] S. Selberherr, "MOS Device Modeling at 77 k," *IEEE Trans. Electron Devices,* vol. 36, no. 8, pp. 1464-1474, Aug. 1989.

[43] Y. Cao, T. Sato, D. Sylvester, M. Orshansky, and C. Hu, *New Paradigm of Predictive MOSFET and Interconnect Modeling for Early Circuit Design,* 2001.

[44] R. Anderson and M. Kuhn, "Low Cost Attacks on Tamper Resistant Devices," *Proc. Int'l Workshop Security Protocols (IWSP '97),* http://citeseer.ist.psu.edu/anderson97low.html, 1997.

[45] S. Mahapatra and M. Alam, "A Predictive Reliability Model for PMOS Bias Temperature Degradation," *Proc. Int'l Electron Devices Meeting (IEDM '02),* Digest, pp. 505-508, 2002.

[46] S. Rangan, N. Mielke, and E. Yeh, "Universal Recovery Behavior of Negative Bias Temperature Instability," *Proc. IEEE Int'l Electron Devices Meeting (IEDM '03),* 8-10, Technical Digest, pp. 14.3.1-14.3.4, Dec. 2003.

[47] M. Denais, V. Huard, C. Parthasarathy, G. Ribes, F. Perrier, N. Revil, and A. Bravaix, "Interface Trap Generation and Hole Trapping under NBTI and PBTI in Advanced CMOS Technology with a 2-nm Gate Oxide," *IEEE Trans. Device and Materials Reliability,* vol. 4, no. 4, pp. 715-722, Dec. 2004.

[48] N. Saxena and J. Voris, "We can remember it for you wholesale: Implications of data remanence on the use of {RAM} for true random number generation on {RFID} tags," *Proc. Workshop on Radio Frequency Identification Security (RFID '09),* July 2009.

Daniel E. Holcomb received the BSECE and MSECE degrees from the University of Massachusetts, Amherst (UMass Amherst). He is currently a graduate student in electrical engineering and computer sciences at the University of California, Berkeley (UC Berkeley). His interests include VLSI, embedded security, and CAD. Prior to graduate work in embedded security, he designed and built embedded systems for analyzing the transport of atmospheric pollution. He has also worked on analyzing and mitigating particle-strike induced soft errors in combinational circuits at UC Berkeley, UMass Amherst, and during two stints as a graduate intern at Intel, Hudson, Massachusetts. He is a student member of the IEEE.

Wayne P. Burleson received the BSEE and MSEE degrees from Massachusetts Institute of Technology (MIT) and the PhD degree in electrical and computer engineering from the University of Colorado. Since 1990, he has been a professor of electrical and computer engineering at the University of Massachusetts, Amherst. He was a custom chip designer for VLSI Technology and Fairchild and a consultant for Digital, Compaq/HP, Intel, Datafusion, and Tensorcomm. He was a visiting professor at ENST, Paris, France in 1996-1997 and at LIRM Montpellier in 2003. His research is in the general area of VLSI, including circuits for low power, long interconnects, clocking and mixed signals, reliability, thermal effects, process variation, and noise mitigation with funding from the US National Science Foundation (NSF), SRC, Compaq/HP, and Intel. He also conducts research in reconfigurable computing, content-adaptive signal processing, embedded security, RFID, and multimedia instructional technologies. He has published more than 100 refereed publications in these areas. He is a member of the ACM, American Society for Engineering Education (ASEE), and Sigma Xi, a senior member of the IEEE, and a former chair of the IEEE Signal Processing Society Technical Committee on Design and Implementation of Signal Processing Systems.

Kevin Fu received the PhD degree in electrical engineering and computer science from Massachusetts Institute of Technology (MIT). He is an assistant professor in the Department of Computer Science, University of Massachusetts, Amherst, where he serves as a director of the RFID Consortium on Security and Privacy (http://RFID-CUSP.org) and a codirector of the Medical Device Security Center (http://secure-medicine.org). His research involves the security and privacy of pervasive technology, including computational RFID, implantable medical devices, and file systems. He received a Sloan Research Fellowship and US National Science Foundation (NSF) Career Award. He is a member of USENIX and the IEEE and a lifetime member of the ACM.